

# Search for $\Upsilon(3S) \rightarrow \pi^0 h_b, h_b \rightarrow \gamma\eta_b$

Lindy Blackburn  
*Physics Department, University of Chicago*

5/23/2003

## Abstract

CLEO III data are analyzed inclusively for evidence of the hadronic decay  $\Upsilon(3S) \rightarrow \pi^0 h_b$  and subsequent radiative transition  $h_b \rightarrow \gamma\eta_b$ . We observe no significant signal for these processes, and thus set the following 90% confidence upper limits:  $\mathcal{B}[\Upsilon(3S) \rightarrow \pi^0 h_b] \leq .116\%$  for an  $h_b$  mass between 9.89 and 9.91 GeV,  $\mathcal{B}[\Upsilon(3S) \rightarrow \pi^0 h_b, h_b \rightarrow \gamma\eta_b] \leq 7.8 \times 10^{-4}$  for an  $h_b$  mass of 9.9 GeV and  $\eta_b$  mass of 9.41 GeV. We also find the possibility of a signal at  $M(h_b) = 9.867$  GeV and  $M(\eta_b) = 9.425$  GeV. If we expand our range of consideration to include this region, we must loosen our upper limits to  $\mathcal{B}[\Upsilon(3S) \rightarrow \pi^0 h_b] \leq .36\%$  and  $\mathcal{B}[\Upsilon(3S) \rightarrow \pi^0 h_b, h_b \rightarrow \gamma\eta_b] \leq 1.43 \times 10^{-3}$  at 90% confidence.

## Introduction

Very few hadronic decays of bottomonia ( $\bar{b}b$ ) have been observed. Other than the  $\pi\pi$  transitions among the vector  $Y(nS)$  states, there have been no such transitions measured. For the isospin-violating single  $\pi^0$  transitions among the vector states, only upper limits appear in the current edition of the Particle Data Group summary.[1] Thus, measurement of hadronic decays in bottomonium would be a significant contribution to our understanding of the physics of heavy quarkonia.

The large number of  $Y(3S)$  events from CLEO III, approximately 4.7 million, makes feasible the investigation of such rare hadronic transitions among the  $Y$  states. Of particular interest is the displacement of the  $h_b(1^1P_1)$  mass from the center of gravity of the well-known triplet  $1^3P_J$  states,  $\chi_{bJ}$ . This measurement would help determine the nature of the confining part of the  $\bar{b}b$  potential.[2] To this date, the only known heavy quarkonium hyperfine splitting is the  $J/\Psi - \eta_c$  mass difference in charmonium.[1]

One of the possible channels in which we can search for the  $h_b$  is the transition  $Y(3S) \rightarrow \pi^0 h_b$  suggested by Voloshin.[3] Voloshin estimates  $\mathcal{B}[Y(3S) \rightarrow \pi^0 h_b] \approx .1\%$ . Rosner and Godfrey also suggest using the photon from the decay  $h_b \rightarrow \gamma \eta_b$ , which has a predicted branching fraction of  $\sim 40\%$ , as a useful tag to narrow in on  $h_b$  events.[4] The previous inclusive-mode upper limit for  $\mathcal{B}[Y(3S) \rightarrow \pi^0 h_b]$  was set at  $.27\%$  for an  $h_b$  mass between 9.89 and 9.91 GeV by the CLEO collaboration using CLEO II data.[5]

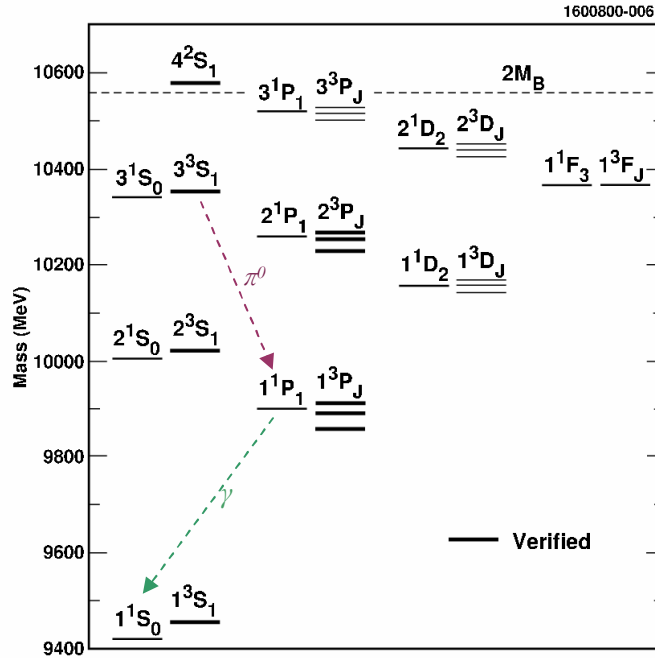


**Figure 1:** The bottomonium energy level spectrum. The singlet states  $h_b(1^1P_1)$  and  $\eta_b(1^1S_0)$  have yet to be seen.

### Single $\pi^0$ Recoil Spectrum

We can first search for the decay process  $Y(3S) \rightarrow \pi^0 h_b, \pi^0 \rightarrow \gamma\gamma$  inclusively by searching the recoil mass spectrum against a single  $\pi^0$  near the expected  $h_b$  mass of 9.9 GeV, the center of

gravity mass of the triplet  $\chi_b(1P)$  states. We subtract weighted sideband regions from the  $\pi^0$  signal region (within 3.5 sigma of the peak of the reconstructed  $\pi^0$  mass) to eliminate all background in the recoil mass spectrum except that from real  $\pi^0$ 's. We then assume a second-order polynomial fit to background and search for a Gaussian  $h_b$  signal between 9.89 and 9.91 MeV with fixed width of 10 MeV as determined from Monte Carlo. We find the greatest yield to be  $-808 \pm 1732$  events from which we obtain  $\mathcal{B}[Y(3S) \rightarrow \pi^0 h_b] \leq .116\%$  at 90% confidence.

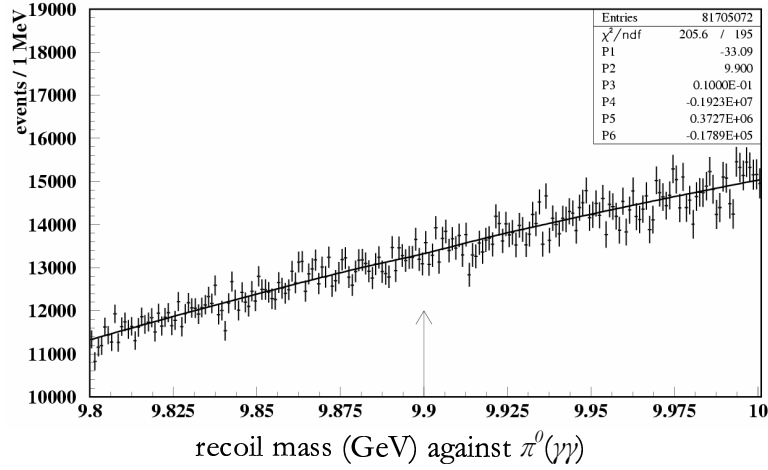


**Figure 2:** Inclusive recoil mass spectrum against a single  $\pi^0$  with a Gaussian fit at 9.9 GeV over smooth background.  $\pi^0$  sidebands are subtracted from the spectrum.

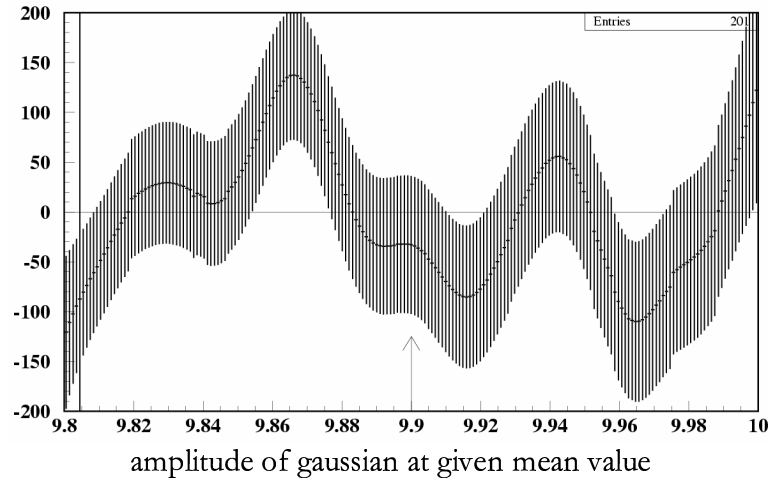


**Figure 3:** The data in figure 2 is fit to a smooth polynomial background plus a Gaussian signal of fixed 10 MeV width and mean value,  $\mu$ . Shown here is the amplitude of the best fit Gaussian as we vary the mean,  $9.8 \leq \mu \leq 10.0$  GeV. Over the region of interest,  $9.89 \leq \mu \leq 9.91$ , the greatest yield for a particular fit is  $-808 \pm 1732$  events.

Because the background from real  $\pi^0$ 's to the single  $\pi^0$  decay is tremendous due to the hadronic nature of the  $Y$  decays, any way to reduce this would be welcome. One method, proposed by Rosner and Godfrey, uses the photon from the daughter decay  $h_b \rightarrow \gamma \eta_b$ , as a

useful tag for events which produce an  $h_b$ [4]. The photon from this decay should have an energy centered just below the  $h_b - \eta_b$  mass difference. Although neither of the singlet states have been experimentally verified, predictions put the  $\eta_b$  mass at  $\sim 9410$  MeV [6], and the  $h_b$  mass should not deviate considerably from the center of gravity mass of the triplet  $\chi_b(1P)$  states, which puts it at  $\sim 9900$  MeV.

This method allows us to look for photons  $\sim 478$  GeV to tag possible events which include an  $h_b \rightarrow \gamma\eta_b$  decay. Because the inclusive photon spectrum falls exponentially with energy, requiring a relatively high energy photon significantly reduces the number of event candidates. The detected photon from  $h_b \rightarrow \gamma\eta_b$  is Doppler shifted up to 20 MeV due to the  $h_b$  momentum. In this analysis we mainly deal with the recoil mass against the photon, which accounts for the kinematics of the decay. Thus, we consider events which have a  $\pi^0$  and also have a photon whose recoil mass is about the expected  $\eta_b$  mass (9.41 GeV).

### Constraints from Decay $h_b \rightarrow \gamma\eta_b$

We search for the decay  $Y(3S) \rightarrow \pi^0 h_b$ ,  $h_b \rightarrow \gamma\eta_b$ , by a similar method as for the inclusive  $Y(3S) \rightarrow \pi^0 h_b$  mode mentioned earlier, except that we consider only events with  $\eta_b$  mass (calculated from the  $\gamma$  recoil) within  $9.41 \pm 40$  MeV, a 2 sigma width as determined by Monte Carlo. To eliminate background from fake  $\pi^0$ 's, where two random photons just happen to have an invariant mass near the  $\pi^0$  mass of 135 MeV, we again subtract  $\pi^0$  sideband regions (2-4 sigma from the peak of the reconstructed  $\pi^0$  mass) from a 2 sigma signal region while plotting the single  $\pi^0$  recoil mass spectrum.

We fit a Gaussian signal of width 10 MeV centered at 9.9 GeV over smooth polynomial background. Using this method gives a yield of  $433 \pm 504$   $h_b$  events, and from this we obtain  $\mathcal{B}[Y(3S) \rightarrow \pi^0 h_b, h_b \rightarrow \gamma\eta_b] \leq 8.8 \times 10^{-4}$ . Our efficiency for  $Y(3S) \rightarrow \pi^0 h_b$  is lowered by 60% however due to our assumption of  $h_b \rightarrow \gamma\eta_b$ . By using this method we obtain  $\mathcal{B}[Y(3S) \rightarrow \pi^0 h_b] \leq .22\%$  at 90% confidence.

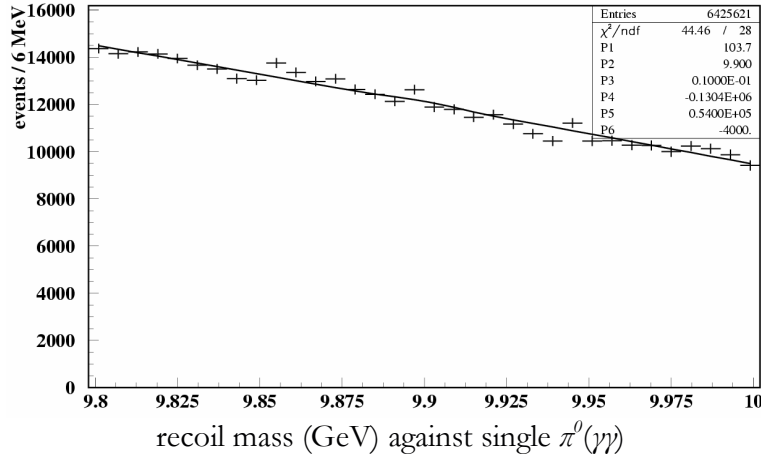


**Figure 4:** Inclusive recoil mass spectrum against a single  $\pi^0$  with a Gaussian fit at 9.9 GeV over smooth background.  $\pi^0$  sidebands are subtracted. Events in this plot must also contain a photon which corresponds to a recoil mass of  $9410 \pm 20$  MeV in context of an  $h_b \rightarrow \gamma\eta_b$  decay.

Using the same analysis, we can also investigate the possibility of seeing the  $\eta_b$  through the decay  $b_b \rightarrow \gamma\eta_b$ . Here we look at the recoil mass spectrum against the photon from  $b_b \rightarrow \gamma\eta_b$  and restrict events such that they have a  $\pi^0$  which is consistent with the production of an  $h_b$  through  $Y(3S) \rightarrow \pi^0 h_b$ . We use the same  $\pi^0$  sideband subtraction as in the previous analysis, and we also subtract an  $h_b$  sideband region (2-4 sigma from 9.9 GeV) from a 2 sigma signal region when plotting the gamma recoil mass. The sideband subtraction on the  $h_b$  is very restrictive since it corresponds to eliminating all sources of background except those which cause an excess in the  $\pi^0$  recoil mass about 9.9 GeV. We fit the heavily subtracted gamma recoil mass spectrum to a smooth polynomial background plus a Gaussian centered at 9.41 GeV with width 14.5 MeV as determined by Monte Carlo. We find a yield of  $377 \pm 332$  events. Our efficiency with these cuts is 22%, from which we obtain  $\mathcal{B}[Y(3S) \rightarrow \pi^0 h_b, h_b \rightarrow \gamma\eta_b] \leq 7.8 \times 10^{-4}$ , and  $\mathcal{B}[Y(3S) \rightarrow \pi^0 h_b] \leq .20\%$  at 90% confidence.

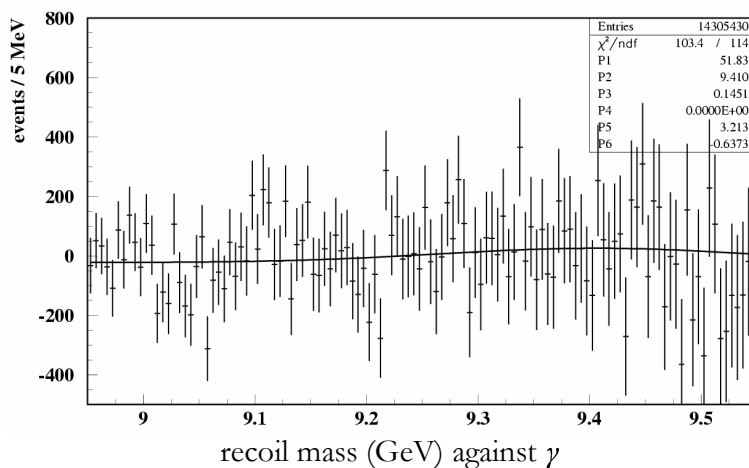


**Figure 5:** Inclusive recoil mass spectrum against a photon from  $b_b \rightarrow \gamma\eta_b$ .  $\pi^0$  and  $h_b$  sidebands are subtracted to yield the final plot. The spectrum is fit to a Gaussian centered at 9.41 GeV over smooth background.

### Broadened Search for $Y(3S) \rightarrow \pi^0 h_b, h_b \rightarrow \gamma\eta_b$

To investigate what happens outside the assumed  $h_b$  window of  $9.89 \leq M(h_b) \leq 9.91$  and to get a better idea of background sources from the inclusive photon spectrum, we look at the  $\gamma$  recoil spectrum for six different  $h_b$  regions each 20 MeV wide, thus covering a range of 9.83 to 9.95 GeV on the single  $\pi^0$  recoil mass. The  $\gamma$  recoil spectra, shown in figure 6, look similar for each of the  $h_b$  regions with no obvious signs of a signal. We use the same technique mentioned earlier and scan the  $\gamma$  recoil spectra searching for possible Gaussian signals of a fixed 19 MeV width. The width is determined by Monte Carlo, but rests on the assumption that the true  $h_b$  mass falls within the center of one of our  $h_b$  regions. Figure 7 shows the results of the scan for signals in the  $\gamma$  recoil spectra. The  $y$ -value represents the amplitude of a best fit Gaussian at each mean value.

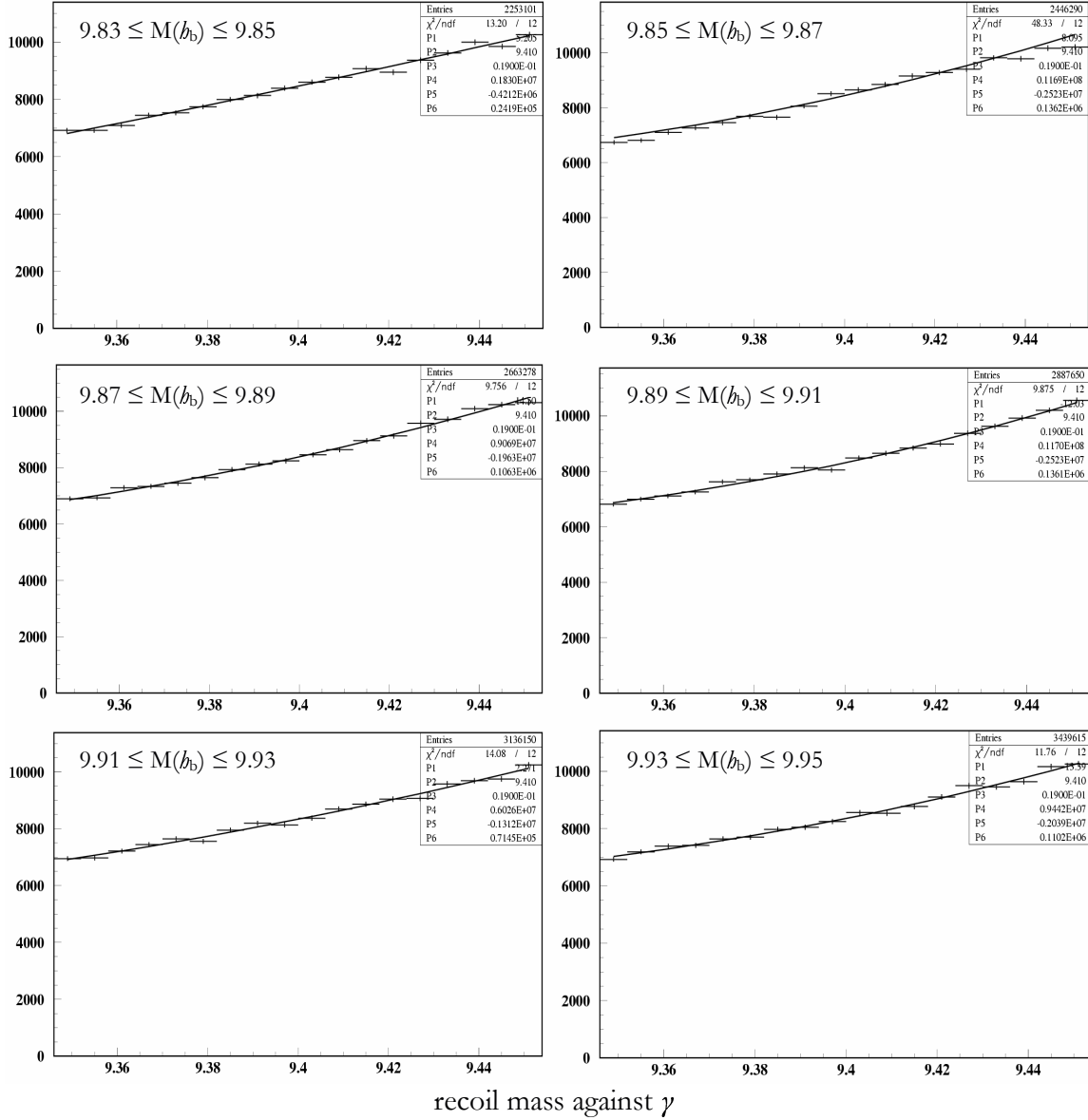


**Figure 6:** Shown here is the  $\gamma$  recoil mass spectrum for six different  $b_b$  regions. Plotted on the  $y$ -axis are the number of events per 6 MeV. The plots are fit to a polynomial background plus Gaussian of fixed 19 MeV width and mean at 9.41 GeV.

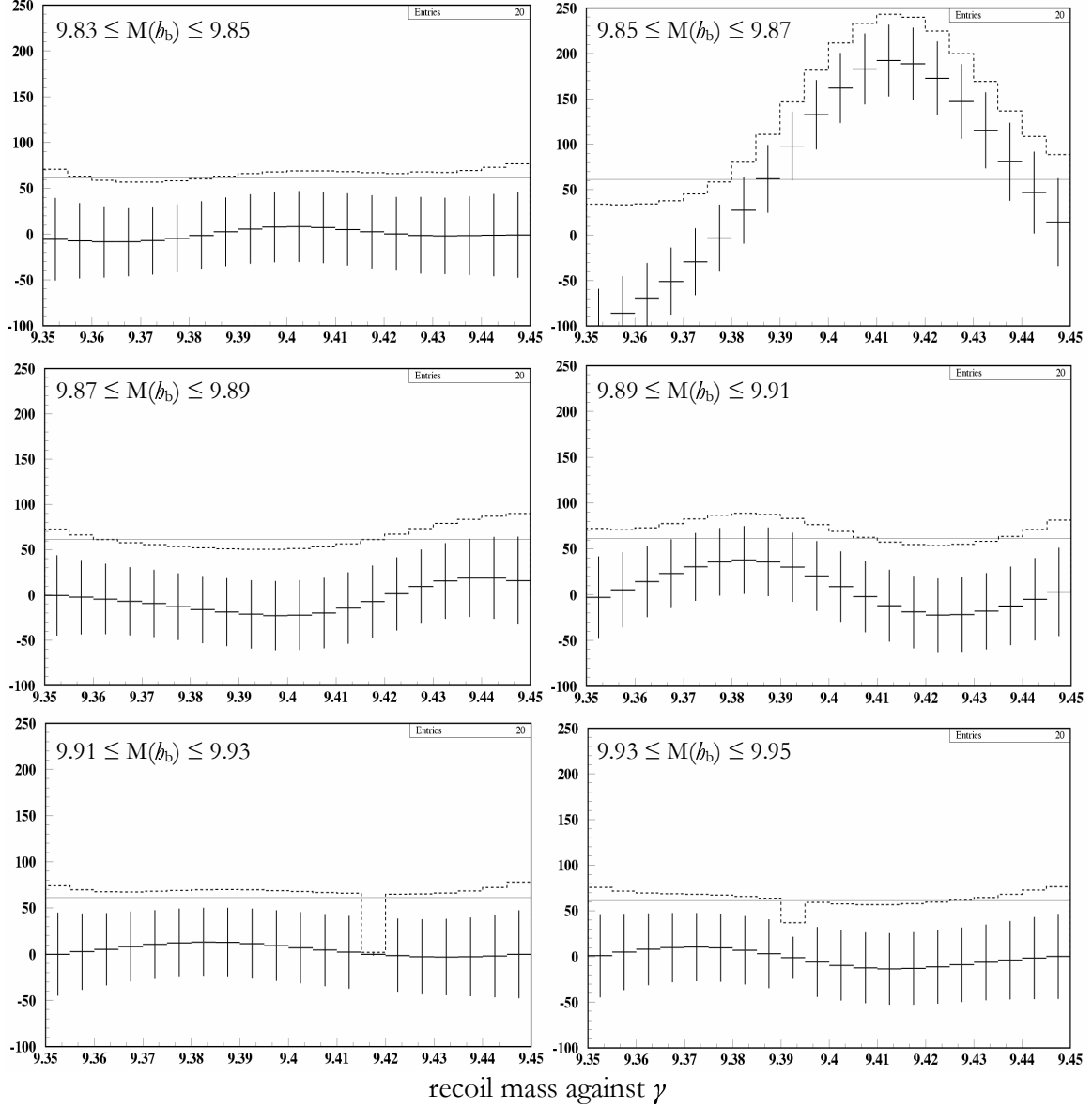


**Figure 7:** The data from figure 6 are fit to polynomial background plus a Gaussian signal of fixed 19 MeV width. Shown here is the amplitude of best fit Gaussian as we vary the mean from 9.35 to 9.45 GeV. The data points with error bars correspond to Gaussian amplitude. The dotted line above corresponds to the resulting 90% upper limit assuming Gaussian likelihood. The straight line is for reference and corresponds to a  $\mathcal{B}[\Upsilon(3S) \rightarrow \pi^0 b_b, b_b \rightarrow \gamma \eta_b] = 4 \times 10^{-4}$ .

The  $\gamma$  recoil spectrum of the  $9.85 \leq M(b_b) \leq 9.87$  region shows considerable deviation from the other regions. The Gaussian of greatest amplitude is fit at a recoil mass of 9413 MeV. It is interesting to note that the single  $\pi^0$  recoil spectrum shows an excess about the same range at  $M(b_b) \approx 9.867$  (see figure 3), although not statistically significant. The photon energy from this decay, however, falls directly into the region of the  $\chi_b(1P)$  radiative transitions:  $\Upsilon(3S) \rightarrow \gamma \chi_b(1P) \rightarrow \gamma \gamma \Upsilon(1S)$ .

We reexamine the data shown in figure 4 and fit to a Gaussian now centered at 9.867 with fixed 10 MeV width and obtain a yield of  $1811 \pm 494$  events. If we assume this to be the  $h_b$ , we calculate  $\mathcal{B}[\Upsilon(3S) \rightarrow \pi^0 h_b, h_b \rightarrow \gamma \eta_b] = 1.06 \times 10^{-3}$ , or  $\mathcal{B}[\Upsilon(3S) \rightarrow \pi^0 h_b, h_b \rightarrow \gamma \eta_b] \leq 1.43 \times 10^{-3}$  at 90% confidence.

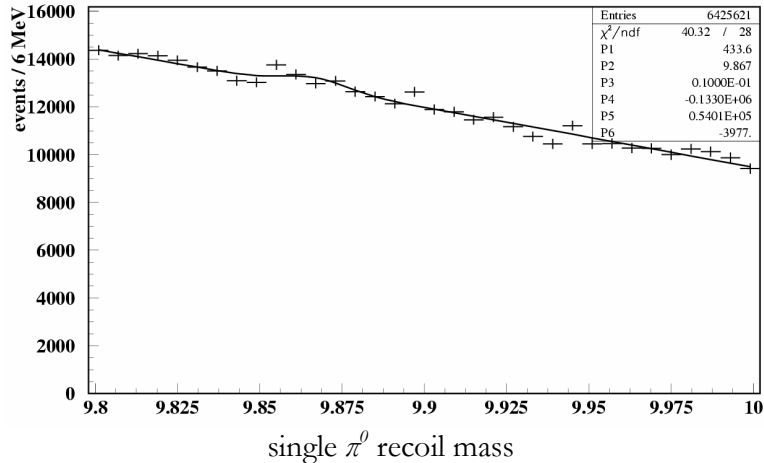


**Figure 8:** Inclusive recoil mass spectrum against a single  $\pi^0$  with a Gaussian fit at 9.867 GeV over smooth background.  $\pi^0$  sidebands are subtracted. Events in this plot must also contain a photon which corresponds to a recoil mass of  $9410 \pm 20$  MeV in context of an  $h_b \rightarrow \gamma \eta_b$  decay.

We use a two-dimensional analysis to investigate further the possibility of a correlated peak in the  $\pi^0$  and  $\gamma$  recoil spectra. Figure 9 shows a plot of  $\pi^0$  recoil versus  $\gamma$  recoil for 5000 signal Monte Carlo events. The signal may be fit to a 2-dimensional Gaussian, with the  $\gamma$  recoil mass coordinate corrected for the direct correlation between assumed  $h_b$  mass and calculated  $\gamma$  recoil mass; thus in the Gaussian,  $x \rightarrow x - y + \mu_y$  where  $x$  represents gamma recoil,  $y$  represent  $\pi^0$  recoil, and  $\mu_y$  is the mean value of the Gaussian in the  $y$  coordinate. Figure 10 demonstrates the resulting fit of the data in figure 9.



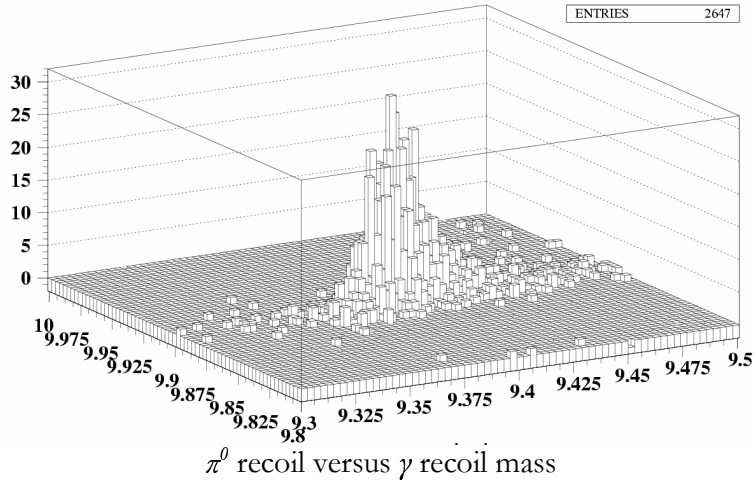


**Figure 9:** Lego-plot representation of  $\pi^0$  recoil versus  $\gamma$  recoil mass for 5000 signal Monte Carlo events. The bin size is  $3 \times 3$  MeV.

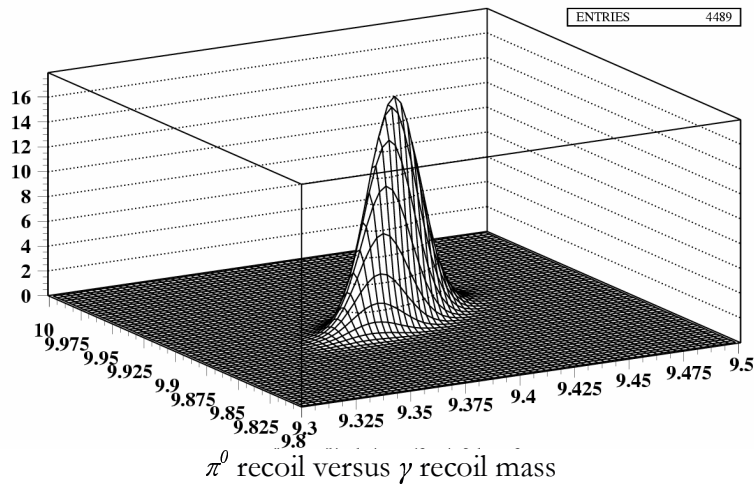


**Figure 10:** 2-dimensional Corrected Gaussian fit to the data in figure 9.

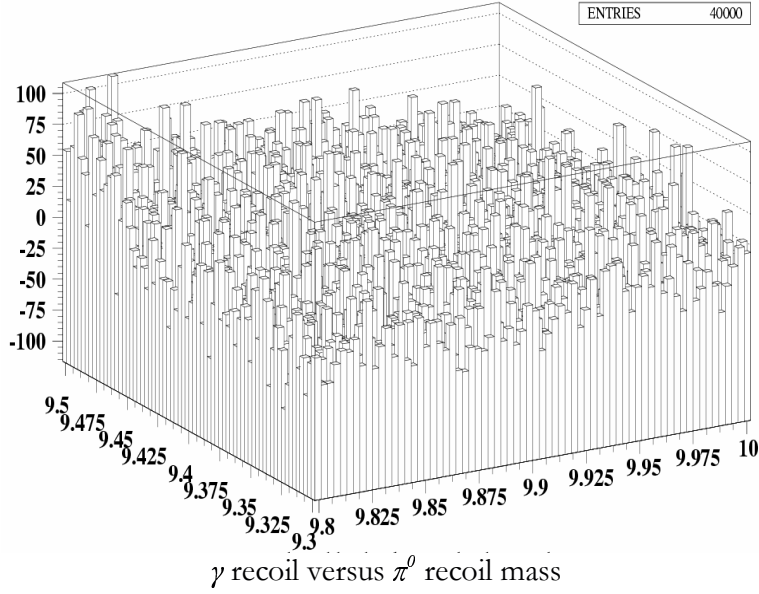


**Figure 11:** A lego-plot representation of the data with polynomial background already subtracted. The bin size is  $3 \times 3$  MeV.

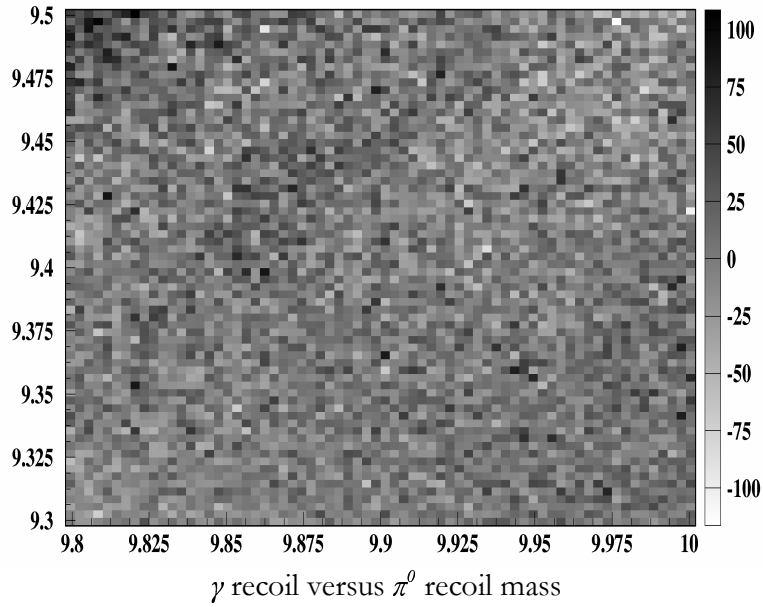
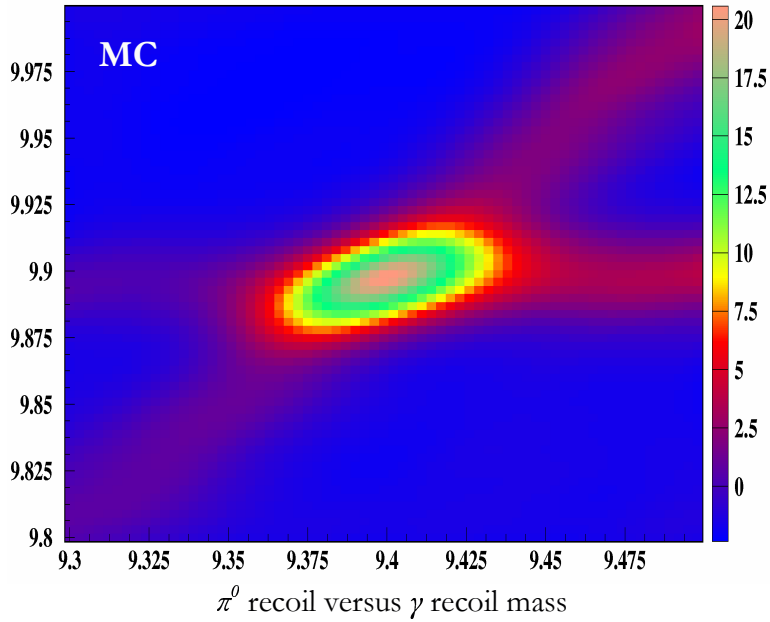
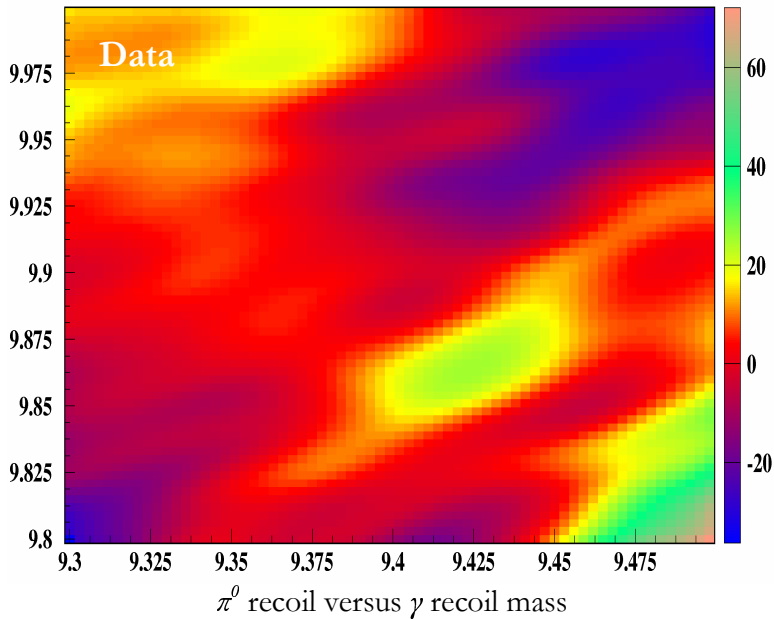


Figure 12: A grey-scale map of the data shown in figure 11.

Using the widths determined by the Monte Carlo fit in figure 10, we can scan through the possible  $b_b$  and  $\eta_b$  masses recording the amplitude of a best fit 2-D Gaussian centered at each particular  $(x, y)$  point representing a specific  $b_b$  and  $\eta_b$  mass. Figure 13 shows a color map of the results of this procedure when it is applied to the signal Monte Carlo shown in figure 9. Figure 14 shows a color map of the results of this procedure when it is applied to the background-subtracted data shown in figures 10 and 11.



**Figure 13:** Gaussian scanning procedure applied to 5000 signal Monte Carlo events. At each  $(x, y)$  point is the amplitude of the best-fit Gaussian to the data in figure 9 centered at  $(x, y)$  and of fixed width according to the fit in figure 10. One can see clearly the effects of the correlation between  $\pi^0$  recoil mass and the resulting  $\gamma$  recoil mass against a photon of certain energy.



**Figure 14:** Gaussian scanning procedure applied to the background-subtracted data. At each  $(x, y)$  point is the amplitude of the best-fit Gaussian to the data in figure 11 centered at  $(x, y)$  and of fixed width according to the fit in figure 10.

In figure 14, we see a distinct excess of events about a  $\pi^0$  recoil mass of  $\sim 9.867$  and an accompanying  $\gamma$  recoil mass of  $\sim 9.425$ , although it does not rise dramatically over background. This shows clearly where the one dimensional behavior shown in figures 6-8 comes from. However, given the overlap of photons from the radiative  $\chi_b(1P)$  transitions, it is difficult to isolate any other signal in the region. The excess in the lower-right corner of the plot, for example, is due to the overwhelming background photons from the  $\chi_b(1P)$  transitions. Still, one would imagine that any structure resulting from  $\chi_b(1P)$  radiative decay would have no effect on the  $\pi^0$  spectrum. What is striking, however, is the resemblance of the peak in question to the Monte Carlo.

### Conclusion

So far the best upper limits on  $\mathcal{B}[Y(3S) \rightarrow \pi^0 b_b]$  are obtained using the straightforward inclusive  $\pi^0$  search. By assuming  $b_b \rightarrow \gamma \eta_b$  one can reduce the background dramatically (almost by a factor of 10) by simply requiring a photon of suitable energy. However, there is much more to be gained by analysis of the  $b_b \rightarrow \gamma \eta_b$  daughter decay than simply elimination of background, as shown by the possibilities of two-dimensional analysis of the compound-decay's phase space. Using such techniques, one might even be able to get around the radiative background from the  $\chi_b(1P)$  states, thus allowing for a more flexible search window.

Although this data shows no statistically significant evidence for the  $b_b$  or  $\eta_b$  states, it would be interesting to see what other  $b_b$  search channels have to offer in the region 9.867 GeV.

### Acknowledgements

I would like to thank my mentor, Jon Rosner, who has guided me through the research for this Bachelor's thesis and to whom I owe a great number of the ideas that kept my work going. I would also like to thank Todd Pedlar who introduced me to High Energy Physics and mentored me over the summer of 2002 while I was an R.E.U. student at Cornell University and began the research from which this project is based. Additionally I would like to thank Matt Shepherd for providing me with generous advice and assistance throughout, and finally the CLEO collaboration and  $b_b$  group for allowing me to participate in their research and for making this work possible.

### VI. References

1. Particle Data Group, D. E. Groom *et al.*, Eur Phys. J. C 14, 1 (2000).
2. See, for example, J. Pantaleone and S.-H. H. Tye, Phys. Rev. D37, 3337 (1988), and V. Gupta and R. Kögerler, Phys. Rev. D37, 740 (1988).
3. M. B. Voloshin, Sov. J. Nucl. Phys. 43, 1011 (1986).
4. S. Godfrey and J. L. Rosner, Phys. Rev. D66, 014012 (2002)
5. F. Butler *et al.*, Phys. Rev. D49, 1 (1994)
6. S. Godfrey and J. L. Rosner, Phys. Rev. D64, 074011 (2001)